The Henryk Niewodniczański
INSTITUTE OF NUCLEAR PHYSICS
Polish Academy of Sciences
152 Radzikowskiego Str., 31-342 Kraków, Poland

www.ifj.edu.pl/reports/2005/

Kraków, February 2005

REPORT No 1958/PN

Monte Carlo simulations of the pulsed thermal neutron flux in two-region hydrogenous systems (using standard MCNP data libraries)

Urszula Wiącek, Ewa Krynicka

Abstract

Monte Carlo simulations of the pulsed neutron experiment in two- region systems (two concentric spheres and two coaxial finite cylinders) are presented. The MCNP code is used. Aqueous solutions of H_3BO_3 or KCl are used in the inner region. The outer region is the moderator of Plexiglas. Standard data libraries of the thermal neutron scattering cross-sections of hydrogen in hydrogenous substances are used. The time-dependent thermal neutron transport is simulated when the inner region has a constant size and the external size of the surrounding outer region is variable. The time decay constant of the thermal neutron flux in the system is found in each simulation. The results of the simulations are compared with results of real pulsed neutron experiments on the corresponding systems.

1. Introduction

Czubek's pulsed neutron method [Czubek *et al.*, 1996] of measuring the thermal neutron macroscopic absorption cross-section Σ_a in small samples is based on a combination of a theoretical approach with experimental results. The theory is based on analytical solutions of the thermal neutron diffusion in a two-region geometry. During measurements the sample-moderator system is irradiated by a burst of 14 MeV neutrons which are slowed down in the system and the thermal neutrons escaping from the system are detected. In consecutive measurements the sample of well-defined and fixed dimensions is enveloped in shells of the moderator of variable thickness and covered with a cadmium shield. A scheme of the experimental set-up is given in Fig. 1. The time decay constant λ of the fundamental mode, $\sim e^{-\lambda t}$, of the pulsed thermal neutron flux in the system is measured. The absorption cross--section Σ_a of the material of the inner sample is interpreted from the measurement results and from the calculation of a certain theoretical curve in such two-region system performed under particular assumptions.

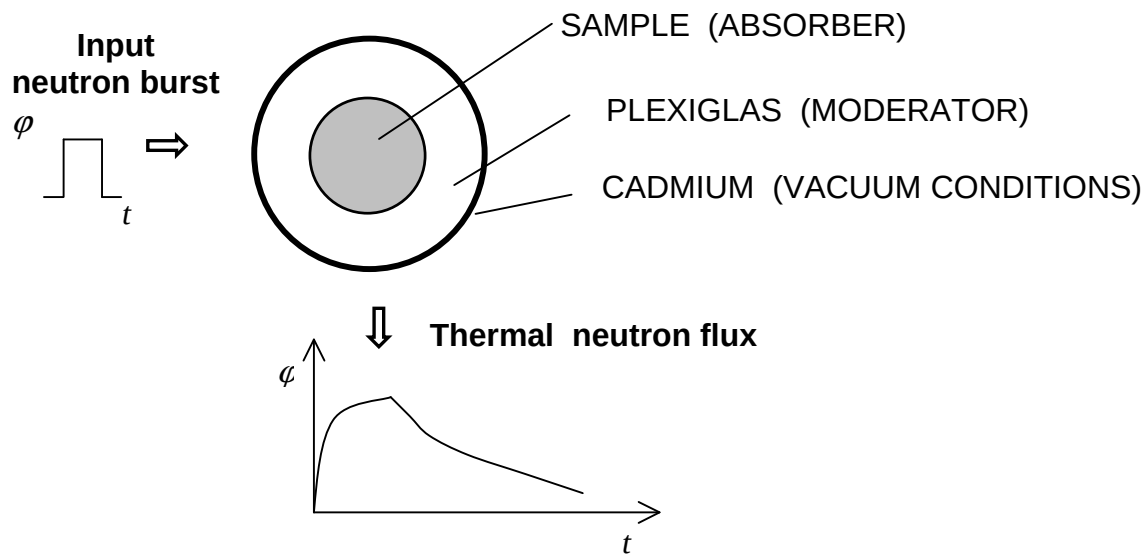

Fig.1. Scheme of the pulsed two-region system.

Materials of a very high purity and, thus, of the exactly known absorption of thermal neutrons are required to verify experimentally the method. It is very difficult to fulfil these requirements and the experimental procedure is time consuming. Computer simulations of the experiments can be very helpful or even can substitute the real measurements. The present work is aimed to compare the results of simulations of the pulsed neutron experiment in Czubek's method by the Monte Carlo method with results of the real experiment and to answer whether these simulations can help in interpretation of difficult experimental cases in

Czubek's method. The simulations have been performed in two-region systems in spherical and cylindrical geometry.

There are various large computational transport codes, as MORSE, FLUKA, MCNP, which use the Monte Carlo method. Only MCNP code allows us to simulate and investigate time-dependent neutron fields. The pulsed neutron experiments were earlier simulated for homogeneous media, as polyethylene [Dąbrowska and Drozdowicz, 2000] and for basic rock minerals [Drozdowicz *et al.*, 2003]. Now, the computer simulations have been performed of the pulsed neutron experiments in two-region geometry like that used in Czubek's method.

2. Hydrogenous moderator

Plexiglas is used in Czubek's method as the outer moderator to obtain a sufficient number of thermal neutrons, which create the thermal neutron field in the investigated system. Plexiglas [poly(methyl methacrylate), $(C_5H_8O_2)_n$] contains hydrogen atoms bound in the molecular system. For most elements the energy-dependent scattering cross-section $\sigma_s(E)$ for thermal neutrons is well described by formula of the free gas model, even for bound atoms. Moreover, it can be often assumed with a sufficient accuracy as a constant, $\sigma_s(E) \approx \sigma_{sf}$, where σ_{sf} is the free atom scattering cross-section. However, this is not the case of a hydrogenous medium because neutron scattering on hydrogen nuclei bound in a molecule is affected by the molecular dynamics, characterised with internal energy modes which are comparable with the incident neutron energies. The scattering cross-section $\sigma_s(E)$ and the average cosine of the scattering angle $\mu(E)$ are then strongly dependent on the incident neutron energy and these dependences are different for different compounds. A single general exact relationship, valid for the energy dependence of the microscopic scattering cross-section $\sigma_s^H(E)$ of hydrogen in various chemical bindings, cannot exist. The individual energy dependence $\sigma_s^H(E)$ for a particular molecule should used.

The pulsed neutron experiment has been simulated by the Monte Carlo method using the MCNP code in which a special procedure is present for transport of thermal neutrons through media containing hydrogen. The standard nuclear data libraries containing the hydrogen scattering cross-sections for neutrons in the thermal energy region exist for a few hydrogenous materials, such as: light and heavy water, methane, benzene, zirconium hydride and polyethylene. Structures of these molecules are simple: H_2O, D_2O, CH_4, C_6H_6, ZrH_2, $(CH_2)_n$, respectively. The Plexiglas macromolecule is more complex. For neutron scattering it contains two types of the hydrogen atoms in the structural formula, considering their neighbourhood. Namely, hydrogen is present in the CH_2 and CH_3 groups. There is no data library for the MCNP code, dedicated especially for hydrogen in Plexiglas.

A procedure which can be adapted to handle by the MCNP the hydrogenous system in Plexiglas is to use the same microscopic data as those for polyethylene, $(CH_2)_n$. This procedure finds the recommendation in comparison of the experimental values of the microscopic scattering cross-sections of hydrogen in Plexiglas obtained by Drozdowicz (1989) and Sibona *et al.* (1991) with those measured in polyethylene by Granada *et al*. (1987). The energy dependence of the total scattering cross-section of hydrogen, $\sigma_s^H(E)$, in Plexiglas and polyethylene is similar although non-identical. Moreover, greater differences can exist between the zero- and first-order energy transfer scattering kernels, $\sigma_0(E \rightarrow E')$ and $\sigma_1(E \rightarrow E')$, in Plexiglas and polyethylene, which influence the average cosine of the scattering angle and the transport cross-section. In spite of this it is interesting to compare the λ_{MCNP} values from the MCNP-simulated experiments with the λ_{exp} values measured in real experiments. The results of the comparison are presented in the paper.

3. Simulated pulsed-neutron experiment

As said, the Monte Carlo method was found very helpful for simulations of the pulsed neutron experiments [Dąbrowska and Drozdowicz, 2000; Woźnicka *et al*., 2000]. The MCNP 4C code [Briesmeister, 2000] has been used here for such simulations.

Neutrons in hydrogenous materials slow down very quickly and they achieve in a short time the Maxwellian energy distribution inside the system. Considering the neutron source, the test was made using once 14 MeV and, second, the Maxwellian distributed thermal neutrons. The results show no influence of the pulsed source type on the determined fundamental decay constant. Therefore, it is possible to use the Maxwellian source in simulations [Dąbrowska and Drozdowicz, 2000; Woźnicka *et al*., 2000], which makes the Monte Carlo calculation significantly faster. Thus, the initial energies of neutrons has been sampled from the Maxwellian source at the room temperature ($E_T = kT = 0.0253$ eV). The thermal neutron source has been isotropic and the neutrons have been uniformly generated inside the sample. The initial position of neutrons has been sampled from the probability density function $p(r) \sim r^2$ for r being inside the entire system. Neutrons have been generated within a 100 μs in width neutron burst. After the neutron burst, the neutron flux in the investigated volume has been scored in 1000 time channels. The width of the channels has been adjusted for each sample individually, depending on the decay rate. The number of histories in the MCNP runs has been chosen for each sample individually to assure the error corresponding to the counting statistics in channels not worse then 0.5%.

After the neutron burst, the flux vanishes in time. Usually it can be recognised as a sum of a number of exponentials and background. We are interested in the decay constant λ of the

fundamental mode, $e^{-\lambda t}$. In order to determine the time decay constant for a given sample, the thermal neutron flux has been scored in time intervals after the source pulse. The decay constant λ of the fundamental mode thermal neutron flux for each sample has been calculated like in a real pulsed experiment [Drozdowicz *et al.*, 1993], including a procedure of the observation of behaviour of the determined value as a function of the delay time.

The relative deviation ε has been defined for comparing the time decay constants from the simulated λ_{MCNP} and real λ_{exp} experiments:

$$\varepsilon\,[\%] = \frac{\lambda_{MCNP} - \lambda_{exp}}{\lambda_{exp}} \cdot 100\,\% \quad . \tag{3.1}$$

Simulations corresponding to the real experiments in spherical [Czubek *et al.,* 1980] and cylindrical [Krynicka *et al.,* 2000a; Krynicka *et al.,* 2001] geometry have been performed. Two kinds of samples have been used: aqueous solutions of boric acid, H_3BO_3, and of potassium chloride, KCl. Their concentrations have been varied to vary the thermal neutron absorption cross-section.

4. Simulations in two-region spherical geometry

The simulations have been performed for the two-region spherical geometry (concentric spheres). The sample of boric acid in light water (H_3BO_3 + H_2O), of the known mass concentration C and the resulting known density ρ, has been surrounded by Plexiglas of density ρ = 1.178 g/cm^3. The radius of the samples has been fixed R_1 = 5.0 cm. The range of the outer radius of Plexiglas has been R_{2g} = (6.5 ÷ 9.49) cm.

The proper selection of MCNP data libraries is an important procedure. Scattering cross--sections for oxygen, boron and carbon have been taken from the ENDF/B-VI.0 standard MCNP data library. For scattering of thermal neutrons on hydrogen the S(α,β) model has been used:

- H in H_2O: TMCCS1, lwtr.01t,
- H in H_3BO_3 is treated as in water,
- H in Plexiglas: TMCCS1, poly.01t (which is for H in polyethylene).

Boron is an element characterising with a high absorption of thermal neutrons. The abundance of the contributing isotopes, ^{11}B and ^{10}B, is very important because their microscopic absorption cross-sections differ extremely. The natural boron isotopic abundance fluctuates slightly [Rosman and Taylor, 1998], which can lead to an uncertainty of the microscopic absorption cross-section σ_{aB}. In this calculations it has been assumed as 20% ^{10}B and 80% ^{11}B according to Mughabghab *et al.* (1981).

The obtained time decay constants of the neutron flux λ_{MCNP} has been compared with the λ_{exp} values known from experiments [Czubek *et al.*, 1980]. The results are listed in Table 1. The standard deviations $\sigma(\lambda)$ of the λ_{exp} and λ_{MCNP} decay constants have been obtained from the variance.

Table 1. Time decay constants λ from the simulated and real experiments in two-region spherical geometry. The H_3BO_3 reference solutions in the inner region.

C	ρ	R_{2g}	λ_{MCNP} $\sigma(\lambda)$	λ_{exp} $\sigma(\lambda)$	ε
[%]	[g/cm^3]	[cm]	[s^{-1}]	[s^{-1}]	[%]
1.75	1.00475	6.5	35 226 24	33 272 486	5.87
				33 311 358	5.75
		7.5	24 468 24	23 357 163	4.76
				23 456 63	4.31
0.875	1.0017	6.5	24 777 51	24 776 112	0.00
				24 771 111	0.02
		6.99	22 210 32	21 286 192	4.34
				21 291 107	4.32
		7.5	19 581 20	18 893 84	3.64
				18 801 106	4.15
		9.49	12 508 4	11 819 182	5.83
				11 829 246	5.74

The average relative deviation ε equals 4.06 %.

The plot λ_{MCNP} *vs* λ_{exp} is shown in Fig. 2. If the results of the simulations and experiments were in a perfect agreement they would lay on the diagonal.

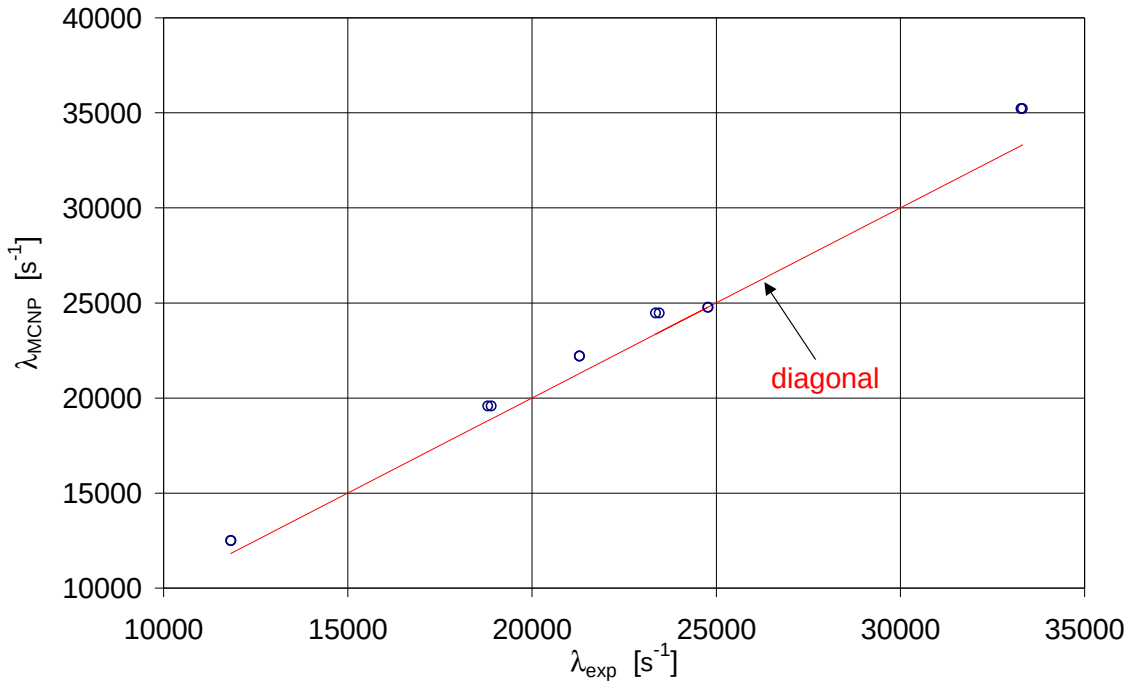

Fig. 2. Decay constant λ_{MCNP} *vs* λ_{exp} in two-region spherical geometry with H_3BO_3 reference solutions in the inner region.

5. Simulations in the two-region cylindrical geometry

The second series of simulations has been performed for the two-region cylindrical geometry (coaxial cylinders). The samples of boric acid in light water (H_3BO_3 + H_2O) and potassium chloride in light water (KCl + H_2O) of the known mass concentrations C and the resulting densities ρ, have been surrounded by Plexiglas of the variable size (H_{2g} = $2R_{2g}$, where H_{2g} and R_{2g} are the external height and radius of the cylinder). The Plexiglas density has been equal ρ = 1.1764 g/cm^3. The size of the samples has been constant (H_1 = $2R_1$ = 6.0 cm) and the range of the outer cylinder radius has been R_{2g} = (4.5 ÷ 7.0) cm.

Scattering cross-sections for oxygen, boron, potassium, chlorine and carbon have been taken from the ENDF/B-VI.0 standard MCNP data library. For scattering of thermal neutrons on hydrogen the S(α,β) model has been used:

- H in H_2O: TMCCS1, lwtr.01t,
- H in H_3BO_3 is treated as in water,
- H in Plexiglas: TMCCS1, poly.01t (which is for H in polyethylene).

The abundances of ^{10}B and ^{11}B for the H_3BO_3 material used in experiments were found in independent measurements [Krynicka *et al.*, 2000b]. They are 19.55% ^{10}B and 80.45% ^{11}B.

The obtained time decay constants of the neutron flux λ_{MCNP} have been compared with the λ_{exp} values known from the experiments [Krynicka *et al.*, 2000a; Krynicka *et al.*, 2001]. The results are listed in Tables 2 and 3. The plot λ_{MCNP} *vs* λ_{exp} is shown in Fig. 3 and Fig. 4.

Table 2. Time decay constants λ from the simulated and real experiments in two-region cylindrical geometry. The H_3BO_3 reference solutions in the inner region.

C	ρ	H_{2g}	λ_{MCNP} $\sigma(\lambda)$	λ_{exp} $\sigma(\lambda)$	ε
[%]	[g/cm^3]	[cm]	[s^{-1}]	[s^{-1}]	[%]
1.0000	1.0022	10.4	22 620 49	22 037 122	2.65
				22 090 184	2.40
				22 102 81	2.34
				22 003 189	2.80
		10.8	21 125 37	20 722 144	1.94
				20 647 97	2.32
				20 625 68	2.42
				20 683 120	2.14
		11.2	19 817 36	19 355 65	2.39
				19 299 88	2.68
				19 367 71	2.32
				19 362 91	2.35
1.1000	1.0025	10.0	24 887 70	24 386 105	2.05
				24 229 80	2.72
				24 297 83	2.43
				24 278 86	2.51
		10.4	23 181 42	22 724 111	2.01
				22 643 119	2.38
				22 630 154	2.43
				22 693 89	2.15
		10.8	21 624 42	21 170 73	2.14
				21 083 84	2.57
				21 050 68	2.73
				21 054 148	2.71
1.2000	1.0029	10.0	25 506 60	25 005 86	2.00
				24 875 112	2.54
				24 945 116	2.25
				24 944 96	2.25
		10.4	23 724 48	23 256 145	2.01
				23 157 173	2.45
				23 222 114	2.16
				23 208 127	2.22
		10.8	22 106 54	21 630 89	2.20
				21 628 85	2.21
				21 808 113	1.37
				21 724 88	1.76
1.4010	1.0036	9.6	28 843 70	28 329 120	1.81
				28 293 81	1.94
				28 403 139	1.55
				28 223 149	2.20

Table 2. (continued)

Table 2. (continued)

C	ρ	H_{2g}	λ_{MCNP} $\sigma(\lambda)$	λ_{exp} $\sigma(\lambda)$	ε
[%]	[g/cm^3]	[cm]	[s^{-1}]	[s^{-1}]	[%]
		10.0	26 706 65	26 177 104	2.02
				26 172 81	2.04
				26 036 164	2.57
				26 094 93	2.35
		10.4	24 710 40	24 235 102	1.96
				24 251 198	1.89
				24 269 196	1.82
				24 144 136	2.34
1.6011	1.0042	9.0	34 448 72	33 413 255	3.10
				33 299 319	3.45
				33 356 329	3.27
				33 341 339	3.32
		9.6	30 322 75	29 662 164	2.23
				29 561 162	2.57
				29 657 140	2.24
				29 513 95	2.74
		10.0	27 934 51	27 216 174	2.64
				27 196 226	2.71
				27 177 154	2.79
				27 190 148	2.74
1.8000	1.0049	9.0	35 928 56	34 696 614	3.55
				34 586 419	3.88

Table 2. (continued)

C	ρ	H_{2g}	λ_{MCNP} $\sigma(\lambda)$	λ_{exp} $\sigma(\lambda)$	ε
[%]	[g/cm^3]	[cm]	[s^{-1}]	[s^{-1}]	[%]
				34 692 517	3.56
				34 684 371	3.59
		9.6	31 420 57	30 676 76	2.43
				30 762 145	2.14
				30 742 101	2.21
				30 705 104	2.33
		10.0	28 856 37	28 155 109	2.49
				28 197 150	2.34
				28 147 116	2.52
				28 129 85	2.58
2.0014	1.0056	8.2	44 942 78	44 019 310	2.10
				43 754 246	2.72
				43 705 430	2.83
				43 680 443	2.89
		8.6	41 063 136	39 823 306	3.11
				39 792 173	3.19
				39 889 594	2.94
				40 411 221	1.61
		9.0	37 407 92	36 705 120	1.91
				36 777 207	1.71

Table 2. (continued)

C	ρ	H_{2g}	λ_{MCNP} $\sigma(\lambda)$	λ_{exp} $\sigma(\lambda)$	ε
[%]	[g/cm^3]	[cm]	[s^{-1}]	[s^{-1}]	[%]
2.1000	1.0060	8.2	45 963 185	45 174 351	1.75
				44 987 206	2.17
				45 065 368	1.99
				45 180 262	1.73
		8.6	41 904 151	41 054 451	2.07
				40 920 268	2.40
				41 150 339	1.83
				40 861 147	2.55
		9.0	37 998 49	37 523 188	1.27
				37 350 163	1.73
				37 512 197	1.30
				37 539 332	1.22
2.2000	1.0063	8.2	47 217 160	46 202 380	2.20
				46 145 236	2.32
				45 902 382	2.86
				45 985 361	2.68
		8.6	42 868 107	41 413 250	3.51
				41 480 383	3.35
				41 318 434	3.75
				41 989 169	2.09
		9.0	38 234 42	37 831 284	1.07
				37 876 211	0.95

Table 2. (continued)

C	ρ	H_{2g}	λ_{MCNP} $\sigma(\lambda)$	λ_{exp} $\sigma(\lambda)$	ε
[%]	[g/cm^3]	[cm]	[s^{-1}]	[s^{-1}]	[%]
				37 910 328	0.85
				37 842 235	1.04
2.3000	1.0067	8.2	48 179 156	46 901 234	2.72
				47 184 219	2.11
				47 142 338	2.20
				47 113 263	2.26
		8.6	43 717 141	42 572 216	2.69
				42 131 260	3.76
				42 602 199	2.62
				42 652 290	2.50
		9.0	39 445 51	38 727 143	1.85
				38 572 131	2.26
2.4000	1.0070	8.2	49 037 100	47 823 239	2.54
				48 184 397	1.77
				47 785 469	2.62
				48 348 386	1.43
		8.6	44 456 134	43 143 162	3.04
				43 258 217	2.77
				42 371 221	4.92
				43 212 285	2.88
				42 642 332	4.25
				42 766 523	3.95

Table 2. (continued)

C	ρ	H_{2g}	λ_{MCNP} $\sigma(\lambda)$	λ_{exp} $\sigma(\lambda)$	ε
[%]	[g/cm^3]	[cm]	[s^{-1}]	[s^{-1}]	[%]
		9.0	40 035 49	38 701 291	3.45
				39 032 274	2.57
				38 569 520	3.80
				38 923 245	2.86
				38 827 136	3.11
				38 920 342	2.86

The average relative deviation ε equals 2.44 %.

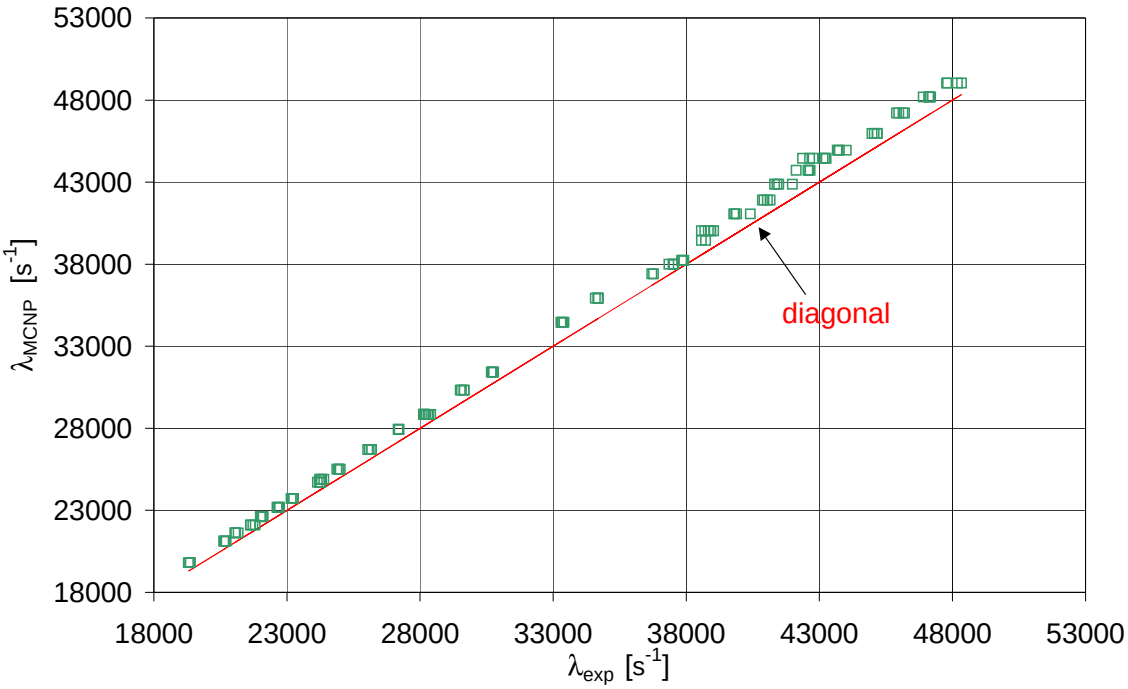

Fig. 3. Decay constant λ_{MCNP} *vs* λ_{exp} in two-region cylindrical geometry with the H_3BO_3 reference solutions in the inner region.

Table 3. Time decay constants λ from the simulated and real experiments in two-region cylindrical geometry. The KCl reference solutions in the inner region.

C	ρ	H_{2g}	λ_{MCNP} σ(λ)	λ_{exp} σ(λ)	ε
[%]	[g/cm^3]	[cm]	[s^{-1}]	[s^{-1}]	[%]
11.500	1.0734	12.8	13 754 29	13 482 23	2.02
				13 494 22	1.93
		13.2	13 153 26	12 887 42	2.06
				12 872 103	2.18
		13.6	12 602 13	12 399 60	1.64
				12 352 38	2.02
		14.0	12 114 18	11 898 50	1.82
				11 885 51	1.93
13.000	1.0836	12.4	14 708 20	14 423 75	1.98
				14 410 46	2.07
				14 428 71	1.94
		12.8	14 022 18	13 757 86	1.93
				13 752 46	1.96
				13 725 52	2.16
		13.2	13 411 25	13 145 84	2.02
				13 144 62	2.03
				13 173 62	1.81
		13.6	12 859 24	12 590 39	2.14
				12 598 63	2.07

Table 3. (continued)

C	ρ	H_{2g}	λ_{MCNP} σ(λ)	λ_{exp} σ(λ)	ε
[%]	[g/cm^3]	[cm]	[s^{-1}]	[s^{-1}]	[%]
				12 574 78	2.27
15.000	1.0974	11.6	16 757 26	16 474 49	1.72
				16 453 39	1.85
				16 416 56	2.08
				16 534 85	1.35
				16 462 97	1.79
				16 534 94	1.35
		12.0	15 866 22	15 595 67	1.74
				15 578 44	1.85
				15 595 59	1.74
				15 583 19	1.82
		12.4	15 109 27	14 764 51	2.34
				14 874 66	1.58
				14 760 84	2.36
				14 889 97	1.48
		12.8	14 399 30	14 125 41	1.94
				14 104 114	2.09
				14 077 50	2.29
				14 162 53	1.67

Table 3. (continued)

C	ρ	H_{2g}	λ_{MCNP} $\sigma(\lambda)$	λ_{exp} $\sigma(\lambda)$	ε
[%]	[g/cm^3]	[cm]	[s^{-1}]	[s^{-1}]	[%]
18.000	1.01185	10.8	19 622 29	19 370 62	1.30
				19 204 37	2.18
		11.2	18 499 28	18 258 110	1.32
				18 254 53	1.34
				18 157 86	1.88
				18 225 128	1.50
		11.6	17 462 22	17 137 53	1.90
				17 185 62	1.61
				17 183 94	1.62
				17 160 59	1.76
		12.0	16 524 22	16 225 50	1.84
				16 232 35	1.80
				16 213 76	1.92
				16 216 32	1.90
		12.4	15 668 13	15 351 46	2.07
				15 344 48	2.11
21.000	1.1401	10.4	21 890 42	21 544 84	1.61
				21 532 67	1.66
				21 547 117	1.59
				21 538 111	1.63

Table 3. (continued)

C	ρ	H_{2g}	λ_{MCNP} $\sigma(\lambda)$	λ_{exp} $\sigma(\lambda)$	ε
[%]	[g/cm^3]	[cm]	[s^{-1}]	[s^{-1}]	[%]
		10.8	20 522 41	20 095 122	2.12
				20 176 90	1.71
				20 157 77	1.81
				20 152 89	1.84
		11.2	19 263 21	18 944 85	1.68
				18 924 77	1.79
				18 883 128	2.01
				18 893 66	1.96
		11.6	18 154 30	17 797 102	2.01
				17 755 100	2.25
				17 812 58	1.92
				17 859 57	1.65
23.600	1.1593	10.0	24 324 44	23 972 59	1.47
				24 079 83	1.02
				23 939 77	1.61
				23 921 104	1.68
		10.4	22 663 26	22 259 98	1.81
				22 334 116	1.47
				22 305 69	1.61
				22 249 104	1.86

Table 3. (continued)

C	ρ	H_{2g}	λ_{MCNP} $\sigma(\lambda)$	λ_{exp} $\sigma(\lambda)$	ε
[%]	[g/cm^3]	[cm]	[s^{-1}]	[s^{-1}]	[%]
		10.8	21 207 29	20 791 76	2.00
				20 787 76	2.02
				20 774 160	2.08
				20 827 71	1.82
		11.2	19 900 32	19 490 37	2.10
				19 512 62	1.99

The average relative deviation ε equals 1.84%.

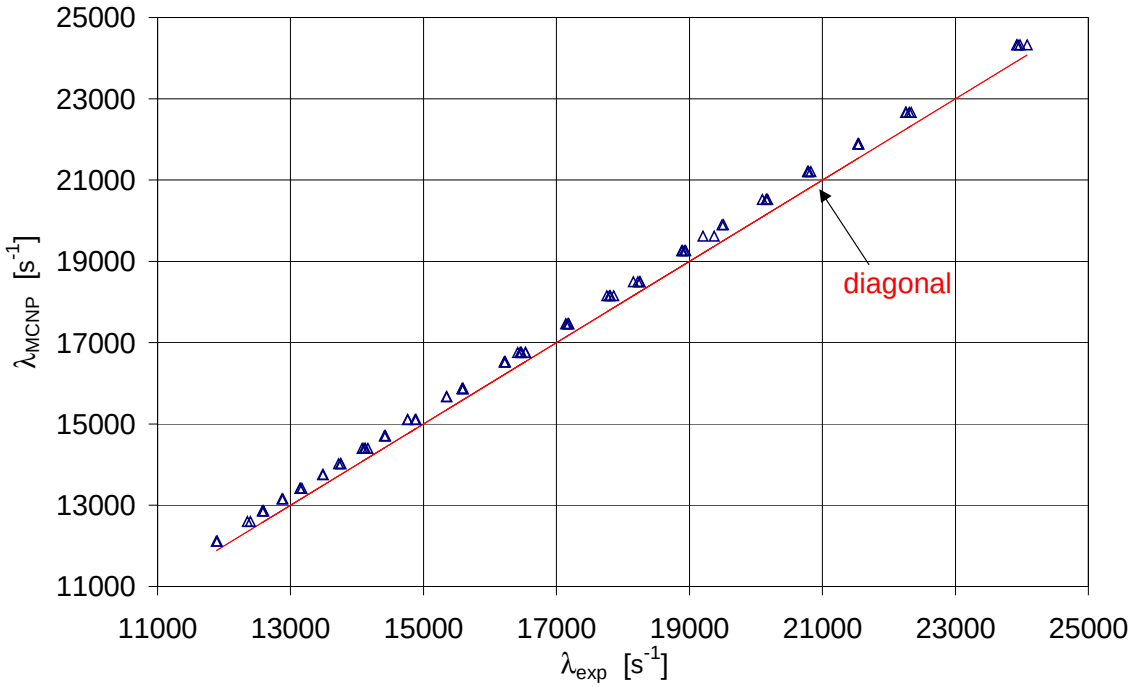

Fig. 4. Decay constant λ_{MCNP} *vs* λ_{exp} in two-region cylindrical geometry with the KCl reference solutions in the inner region.

The useful range of the time decay constants λ in Czubek's method covers the interval 12 000 $s^{-1} \leq \lambda \leq$ 50 000 s^{-1}. It can be achieved when both reference materials (the aqueous solutions of H_3BO_3 and KCl) are taken into account. The time decay constants λ_{MCNP} *vs* λ_{exp} for both materials together are plotted in Fig.5. The average relative deviation ε equals 2.20%.

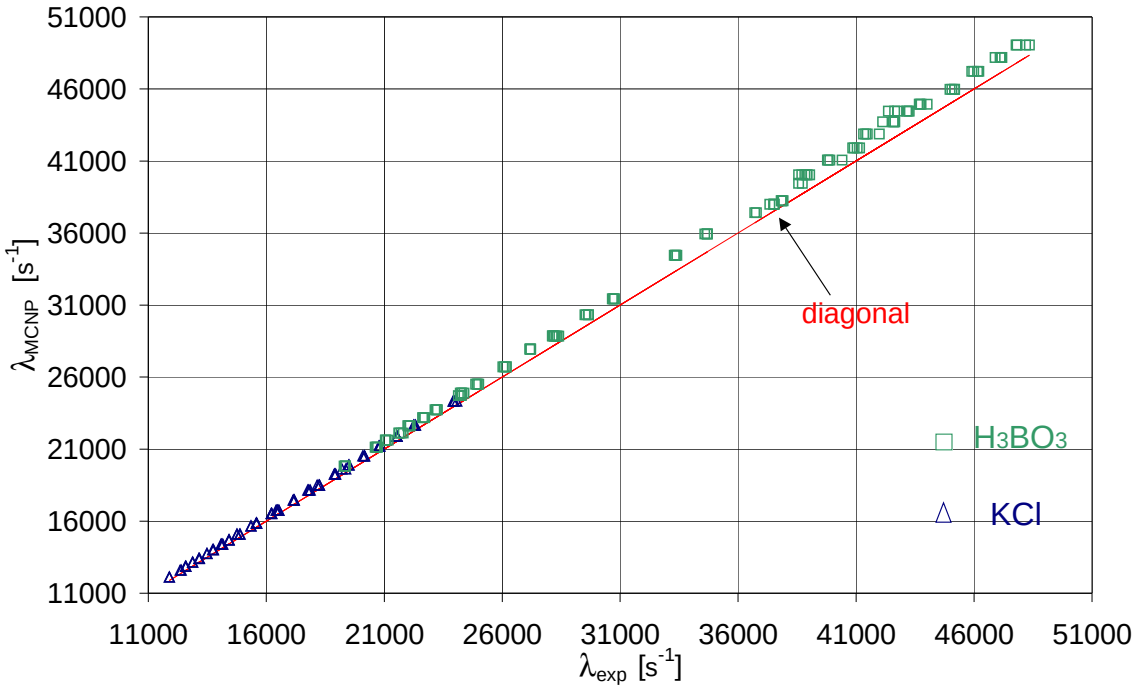

Fig. 5. Decay constant λ_{MCNP} *vs* λ_{exp} in two-region cylindrical geometry (H_3BO_3 or KCl reference solutions in the inner region).

6. Conclusions

The performed calculations have allowed us to obtain the routine way of computer simulations of the pulsed neutron experiments in two-region geometry like that used in Czubek's method. The fundamental decay constants λ_{MCNP} of the thermal neutron flux have been compared with the λ_{exp} values measured in real experiments.

A few experiments made in the overlapping intervals of the absorption resulting from the H_3BO_3 and KCl solutions show a very good conformity of the results. In all cases the λ_{MCNP} values are greater than the λ_{exp} values. The maximum relative deviation ε between these values has been equal to 5.87%. The average deviation in the two-region cylindrical geometry has been ca. 2%. The most probable reason of this behaviour comes from the use in the simulations the scattering library of hydrogen in polyethylene recommended for hydrogen in Plexiglas (as there is no separate library for the latter material). An improvement of this library is necessary for more precise quantitative calculations.

References

Briesmeister J. F. (2000)
Monte Carlo N-Particle Transport Code System. Version 4C.
LA–13709–M, Los Alamos National Laboratory.

Czubek J. A., Drozdowicz K., Gabańska B., Igielski A., Krynicka E., Woźnicka U. (1996)
Thermal neutron macroscopic absorption cross-section measurement applied for geophysics.
Progr. Nucl. Energy **30**, 295-303.

Czubek J. A., Drozdowicz K., Igielski A., Krynicka-Drozdowicz E., Sobczyński Z., Woźnicka U. (1980)
Thermal neutron absorption cross-section for small samples (Experiments in spherical geometry).
Rept. INP No. 1119/AP, Institute of Nuclear Physics, Kraków.

Dąbrowska J., Drozdowicz K. (2000)
Monte Carlo simulation of pulsed neutron experiments on samples of variable mass density.
Nucl. Instrum. Meth. **A 443**, 416-421.

Drozdowicz K. (1989)
Total cross-section of Plexiglass in the thermal neutron region.
Ann. Nucl. Energy **16**, 275-278.

Drozdowicz K., Gabańska B., Krynicka E. (1993)
Fitting the decaying experimental curve by sum of exponentials.
Rept. INP No. 1635/PM, Institute of Nuclear Physics, Kraków.

Drozdowicz K, Krynicka E., Dąbrowska J. (2003)
Diffusion cooling of thermal neutrons in basic rock minerals by Monte Carlo simulation of the pulsed neutron experiments.
Appl. Radiat. Isot. **58**, 727-733.

Granada J. R., Dawidowski J., Mayer R. E., Gillette V. H. (1987)
Thermal neutron cross-section and transport properties in polyethylene.
Nucl. Instrum. Meth. **A 261**, 573-578.

Krynicka E., Drozdowicz K., Gabańska B., Janik W., Dąbrowska J. (2000a)
Measurements of the thermal neutron absorption Σ_a of model systems (reference KCl solutions) in two–region geometry.
Rept. INP No. 1857/PN, Institute of Nuclear Physics, Kraków.
http://www.ifj.edu.pl/reports/2000.

Krynicka E., Gabańska B., Woźnicka U., Dąbrowska J., Burda J. (2001)
Interpretation problems of Czubek's Σ_a measurements method. Reference experiment on H_3BO_3 solutions.
Rept. INP No. 1890/PN, Institute of Nuclear Physics, Kraków.
http://www.ifj.edu.pl/reports/2001.

Krynicka E., Gabańska B., Woźnicka U., Kosik M. (2000b)
Measurements of the thermal neutron absorption Σ_a of boron of unknown isotopic ratio.
Rept. INP No. 1860/PN, Institute of Nuclear Physics, Kraków.
http://www.ifj.edu.pl/reports/2000.

Mughabghab S. F., Divadeenam M., Holden W. E. (1981)
Neutron cross-sections, vol.1. Neutron resonance parameters and thermal cross-sections Part A: Z = 1 – 60.
Academic Press, New York.
Rosman K. J. R., Taylor P. D. P. (1998)
Isotopic compositions of the elements 1997.
Pure & Appl. Chem. **70**, 217-235.
Sibona G., Mayer R. E., Gillette V. H., Bonetto C., Granada J. R. (1991)
Thermal neutron cross-sections and diffusion parameters of Plexiglass.
Ann. Nucl. Energy **18**, 689-696.
Woźnicka U., Drozdowicz K., Dąbrowska J. (2000)
A generalised interpretation of buckling experiments for thermal neutrons.
Nucl. Instrum. Meth. **A 455**, 660-669.